A Linear AC Power-Flow-Based Cascading Failure Model Balancing Accuracy and Efficiency

1st Zhengyang Jin
School of Electrical Engineering
Xi'an Jiaotong University
Xi'an, China
17839870620@163.com

2nd Jiapeng Li
School of Electrical Engineering
Xi'an Jiaotong University
Xi'an, China
jiapengli@xjtu.edu.cn

3rd Le Liu
School of Electrical Engineering
Xi'an Jiaotong University
Xi'an, China
liule@xjtu.edu.cn

4th Xuming Chen
School of Electrical Engineering
Xi'an Jiaotong University
Xi'an, China
chenxuming@stu.xjtu.edu.cn

5th Xiaoning Kang
School of Electrical Engineering
Xi'an Jiaotong University
Xi'an, China
kangxn@xjtu.edu.cn

6th Yujun Li
School of Electrical Engineering
Xi'an Jiaotong University
Xi'an, China
yujunli@xjtu.edu.cn

***Abstract*—Cascading failures in power systems involve discrete actions of numerous protection and security automation control equipment, and frequent topology changes, making a closed-form mathematical description intractable. High-fidelity AC simulations are computationally prohibitive for large systems, limiting their use in practical contingency assessment and mitigation design. This paper proposes a linear AC power-flow-based cascading failure model that achieves a balance between accuracy and computational efficiency. Leveraging typical voltage operating ranges and the structural properties of the admittance matrix, a simplified linear AC power-flow model is derived. This formulation retains a linear form similar to that of DC power flow, greatly accelerating power flow transfer calculations. Meanwhile, it preserves voltage and reactive power characteristics, achieving minimal errors compared to conventional AC power flow. Building on this, a cascading failure model that encodes realistic protection and security automation logic is developed, including overload tripping, under-voltage load shedding, frequency regulation, and operator actions. The proposed model faithfully reproduces load-shedding triggered by voltage and frequency violations during fault propagation, avoiding the uniform or OPF-based load shedding heuristics commonly invoked to resolve AC power flow non-convergence. This yields faster, convergence-robust simulations without sacrificing the key physics needed for credible blackout risk assessment.**

***Index Terms*—Cascading failures, liner AC power flow model, security automatic equipment, power system resilience**

I. Introduction

Ongoing climate change is placing excessive strain on the environment, resulting in an ever-increasing frequency and intensity of extreme weather events (EWEs) [1]. Power systems, one of the most widespread and critical infrastructures, have been seriously affected by EWEs in recent decades, causing widespread blackouts and substantial economic losses. Blocking cascading failures, a major cause of blackouts, is considered a crucial means of enhancing system resilience [2].

Cascading failure models are a class of models that realistically simulate system dynamics under fault threats. Traditional cascading failure models, such as OPA model [3], offer strong insight into self-organized criticality (SOC) of systems over long-term evolution, but neglects system behavior during fast cascading stage. To more precisely characterize this stage, researchers have developed dynamic models, such as the COSMIC model [4] and dynamic PRA model [5], via differential-algebraic equations. while these models provide a more detailed depiction of cascading failures, their substantial computational burden conflicts with the need for timely large-scale multi-scenario contingency assessment and mitigation design in practical engineering projects [6].

Simulating cascading failures in power systems requires balancing accuracy and efficiency, which respectively ensure the precision and timeliness of mitigation actions. Since protection systems governing cascading failures are designed for steady-state operation, static power-flow-based models provide sufficient accuracy. Reference [7] compared cascading processes under dynamic and static models, finding close agreement prior to system collapse. Reference [8] showed that a static model, when calibrated via internal parameter adjustments, can yield results comparable to those of dynamic models.

However, static models suffer from convergence issues under drastic topological changes. Existing approaches to non-convergence are highly constrained and often compromise simulation fidelity through artificial interventions [9]. Reference [10] treat non-convergence as a system failure, using it as a termination condition. Reference [11] attempts OPF-based load shedding in non-convergence scenarios, which overlooks actual physical process. Moreover, the use of optimization algorithms slow the simulation and introduce uncontrollable factors [12], casting doubt on simulation authenticity.

To balance accuracy and efficiency, this paper proposes a linear AC power flow method that reliably converges and yields minimal errors for cascading failure simulation, while

This research was supported by National Key R&D Program of China (2024YFC3015100).

979-8-3315-8138-1

eliminating time losses from optimization routines or repeated AC power-flow iterations. Building on this, a cascading failure model that encodes realistic protection and security automatic control equipment is developed, faithfully reproducing load-shedding triggered by voltage and frequency violations.

The remainder of this paper is organized as follows: Section II derives the proposed linear AC power flow; Section III develops the cascading failure model with protection and control mechanisms; Section IV evaluates the proposed power flow and demonstrates the features of the cascading failure model; Section V draws conclusions.

II. Derivation of the Linear AC Power Flow

The DC power flow model that neglects voltage deviation has been widely adopted for its ability to approximate AC power flow. However, in real power systems, voltage and reactive power exert significant influence on grid operation. Moreover, relay protection and security automatic control equipment, such as under-voltage load shedding (UVLS), depend on bus voltage magnitudes for action decisions, making voltage a critical variable in cascading-failure studies.

Conventional iterative methods for solving AC power flow often exhibit low efficiency or even non-convergence, especially under drastic topological changes. To enhance robustness, power-flow-based cascading-failure models typically resort to uniform or OPF-based load shedding, thereby neglecting the logic of actual control equipment. To address this, this paper proposes a linear AC power flow model that avoids convergence issues and enables faster, more precise simulation of security automatic control actions

The traditional AC power flow equations are given in (1).

$$\begin{cases} P_i = U_i \sum_{j=1}^{N_{bus}} \left(G_{ij} U_j \cos\theta_{ij} + B_{ij} U_j \sin\theta_{ij} \right) \\ Q_i = U_i \sum_{j=1}^{N_{bus}} \left(G_{ij} U_j \sin\theta_{ij} - B_{ij} U_j \cos\theta_{ij} \right) \end{cases} \tag{1}$$

where N_{bus} is the total number of buses in the system; P_i and Q_i are the injected active and reactive power at bus i; U_i is the voltage magnitude at bus i; θ_{ij} is the voltage angle difference between bus i and j; G_{ij} and B_{ij} are respectively real and imaginary parts of the bus admittance element Y_{ij}.

For the vast majority of stable operating scenarios, the bus voltage magnitudes remain close to 1 p.u., and the absolute voltage phase angle differences are typically within 30° [13]. These characteristics justify the following approximations: $U_i \approx U_j$, $\cos\theta_{ij} \approx 1$, $\sin\theta_{ij} \approx \theta_i - \theta_j$. Furthermore, consider the inherent structure of the admittance matrix, shown in (2).

$$Y_{ij} = \begin{cases} -\left(g_{ij} + jb_{ij}\right) & \text{if} \quad j \neq i \\ g_{ii} + jb_{ii} + \sum_{k=1,k\neq i}^{N_{bus}} \left(g_{ik} + jb_{ik}\right) & \text{if} \quad j = i \end{cases} \tag{2}$$

where g_{ij} and b_{ij} are the real and imaginary parts of admittance between bus i and bus j; g_{ii} and b_{ii} are the real and imaginary parts of the shunt admittance at bus i.

By substituting the assumptions regarding voltage and trigonometric functions, combined with the admittance matrix structure (2), into (1), we ultimately derive (3)-(4), with the detailed derivation for active power listed.

$$\begin{aligned} P_i &= g_{ii} U_i^2 + \sum_{j=1,j\neq i}^{N_{bus}} \Big(g_{ij} U_i \big(U_i - U_j \cos\theta_{ij} \big) - b_{ij} U_i U_j \sin\theta_{ij} \Big) \\ &\approx g_{ii} U_i + \sum\nolimits_{j=1,j\neq i}^{N_{bus}} \Big(g_{ij} \big(U_i - U_j \big) - b_{ij} \big(\theta_i - \theta_j \big) \Big) \\ &= U_i \sum_{j=1}^{N_{bus}} g_{ij} + \sum_{j=1,j\neq i}^{N_{bus}} (-g_{ij}) U_j - \theta_i \sum_{j=1,j\neq i}^{N_{bus}} b_{ij} - \sum_{j=1,j\neq i}^{N_{bus}} (-b_{ij})\, \theta_j \\ &= \sum_{j=1}^{N_{bus}} G_{ij} U_j - \sum_{j=1}^{N_{bus}} \tilde{B}_{ij} \theta_j \end{aligned} \tag{3}$$

$$Q_i = -\sum_{j=1}^{N_{bus}} B_{ij} U_j - \sum_{j=1}^{N_{bus}} \tilde{G}_{ij} \theta_j \tag{4}$$

where $\tilde{G}$ and $\tilde{B}$ denote the real and imaginary parts of the bus admittance matrix with shunt admittance neglected.

Because different buses have different control variables, buses are classified into three types: $U\theta$, PU, and PQ. Based on this classification, (3)-(4) are partitioned into block-matrix form, using R, G, and D to respectively label $U\theta$, PU, and PQ buses. Through algebraic rearrangement, the detailed calculation formulas are established in (5)-(8). Specifically, (5)-(7) are employed to determine the actual state variables, while (8) is used to back-calculate the reference bus phase angle and compensate the global voltage phase angle offset, via $\theta - \theta_R$. Applying the same simplifications, the branch power flow equations are similarly simplified into a linear form, as given in (9).

$$\begin{bmatrix} \tilde{P}_G \\ \tilde{P}_D \\ \tilde{Q}_D \end{bmatrix} = \begin{bmatrix} P_G \\ P_D \\ Q_D \end{bmatrix} + \begin{bmatrix} \tilde{B}_{GR} & -G_{GR} & -G_{GG} \\ \tilde{B}_{DR} & -G_{DR} & -G_{DG} \\ \tilde{G}_{DR} & B_{DR} & B_{DG} \end{bmatrix} \begin{bmatrix} \theta_R \\ U_R \\ U_G \end{bmatrix} \tag{5}$$

$$\begin{bmatrix} \theta_G \\ \theta_D \\ U_D \end{bmatrix} = - \begin{bmatrix} \tilde{B}_{GG} & \tilde{B}_{GD} & -G_{GD} \\ \tilde{B}_{DG} & \tilde{B}_{DD} & -G_{DD} \\ \tilde{G}_{DG} & \tilde{G}_{DD} & B_{DD} \end{bmatrix}^{-1} \begin{bmatrix} \tilde{P}_G \\ \tilde{P}_D \\ \tilde{Q}_D \end{bmatrix} \tag{6}$$

$$\begin{aligned} \begin{bmatrix} Q_R \\ Q_G \end{bmatrix} &= - \begin{bmatrix} \tilde{G}_{RR} & \tilde{G}_{RG} & \tilde{G}_{RD} \\ \tilde{G}_{GR} & \tilde{G}_{GG} & \tilde{G}_{GD} \end{bmatrix} \begin{bmatrix} \theta_R \\ \theta_G \\ \theta_D \end{bmatrix} \\ &\quad - \begin{bmatrix} B_{RR} & B_{RG} & B_{RD} \\ B_{GR} & B_{GG} & B_{GD} \end{bmatrix} \begin{bmatrix} U_R \\ U_G \\ U_D \end{bmatrix} \end{aligned} \tag{7}$$

$$\begin{aligned} \theta_R = \tilde{B}_{RR}^{-1} \big(& \mathbf{1}^{\mathrm{T}} P_G + \mathbf{1}^{\mathrm{T}} P_D - \tilde{B}_{RG} \theta_G - \tilde{B}_{RD} \theta_D \\ & + G_{RR} U_R + G_{RG} U_G + G_{RD} U_D \big) \end{aligned} \tag{8}$$

$$\begin{cases} P_{ij} \approx g_{ij} \big(U_i - k_{ij} U_j \big) / k_{ij}^2 - b_{ij} \big(\theta_i - \theta_j - \theta_{ij}^k \big) / k_{ij} \\ Q_{ij} \approx -b_{ij} \big(U_i - k_{ij} U_j \big) / k_{ij}^2 - g_{ij} \big(\theta_i - \theta_j - \theta_{ij}^k \big) / k_{ij} \end{cases} \tag{9}$$

where $\tilde{P}$ and $\tilde{Q}$ are auxiliary injected active and reactive powers; P_{ij} and Q_{ij} are active and reactive power flows from bus i to bus j; k_{ij} and θ_{ij}^k denote the transformation ratio and phase-shifting angle between bus i and bus j.

The proposed linear AC power flow model exploits typical operating ranges and structural properties of the bus admittance matrix to preserve accurate voltage estimates after linearization. The resulting calculation matrices retain the

979-8-3315-8138-1

canonical form of the bus admittance matrix, making them easy to update, typically non-singular and highly sparse, ultimately ensuring stable and fast calculations.

III. Linear AC Power-flow-based Cascading Failure Model

A. Modeling of Protection and Control Mechanisms

Cascading failures are inherently complex processes, in which a small initial perturbation can trigger a sequence of subsequent outages. In practice, the actual disconnection actions are executed by relay protection. Likewise, certain control mechanisms can play a crucial role. Therefore, detailed modeling of protection and control mechanisms is essential for credible simulation of cascading failures. The following will introduce the key mechanisms and corresponding simulation methods for several representative phenomena.

1) Under-voltage: When bus voltage fall below a certain threshold, UVLS sheds load sequentially to avert voltage collapse. Prior cascading failure studies based on AC power flow often faced convergence issues, forcing the use of uniform load shedding or OPF-based load shedding that are independent with the real physics process. Especially in DCOPF-based models, the multiplicity of linear programming solutions further introduces uncontrollable factors [12]. the proposed model leverages the linear AC power flow model to eliminate convergence problems. Combined with iterative UVLS, it delivers fast and robust convergence under abnormal operating conditions, preserving the physical consistency of voltage-driven shedding behavior.

2) Overload: Overload propagation is widely viewed as a key driver in cascading failures. In practice, line tripping can be initiated by several protections, including distance protection (DP), dynamic line rating protection (DLRP) and so on. Equation (10) is considered as a unified disconnection criterion that consistently evaluates the combination of line thermal capacity, pre-contingency operating state, and post-contingency state.

$$\alpha = \arg\max_{\alpha \in \mathcal{L}} \left(\frac{f_\alpha - f_\alpha^0}{f_\alpha^{\mathrm{st}}} \exp\left(\frac{f_\alpha - f_\alpha^{\mathrm{st}}}{f_\alpha^{\mathrm{st}}} \right) \right) \tag{10}$$

where α is the index of the branch selected for disconnection; $\mathcal{L}$ is the set of all branch indices; f_α, f_α^0, f_α^{st} denote post-contingency power flow, pre-contingency power flow and short-term capacity of branch α, respectively.

3) Over-frequency and under-frequency: Power-system components require a stable frequency, motivating a suite of frequency-control mechanisms such as automatic generation control (AGC) and under-frequency load shedding (UFLS). Considering the disparate response time scales between primary frequency control (PFC) and AGC, the maximum frequency deviation is estimated considering only PFC operating, as expressed in (11). Specifically, different thresholds are set to control the startup of AGC, generation protection (GP), PFC and UFLS [14]. The corresponding startup conditions and modeling mechanisms for these devices are shown in Tab. I.

$$\Delta f = \frac{-\sum_{g\in\Omega_G} P_g + \left(\sum_{d\in\Omega_D} P_d + \sum_{b\in\Omega_B} P_b \right)}{\sum_{g\in\Omega_G} 1/R_g + \sum_{d\in\Omega_D} D_d} \tag{11}$$

where Ω_G, Ω_D are respectively sets of buses with generation and load; Ω_B is the set of branches; P_g, P_d are respectively active power injection at bus g and d; P_b is the active power loss on branch b; R_g is the adjustment coefficient at bus g; D_d is the power regulation coefficient at bus d.

TABLE I
Frequency Recovery Strategy

Devices	**Thresholds and Operational mechanisms**	
	Startup conditions	***Modeling mechanisms***
AGC	$\lvert\Delta f\rvert \geq 0.2$Hz	AGC units adjust outputs proportionally based on reserves
UFLS	$\Delta f \leq -1$ Hz	Load shedding across the entire network until frequency is restored
GP	$\Delta f \leq -2.5$ Hz or $\Delta f \geq 1.5$ Hz	Trip based on reserve gap[a] and frequency
PFC	$\lvert\Delta f\rvert \leq 0.2$Hz	Generations adjust output based on R_g

[a]Determined by subtraction between unbalanced power and total reserve.

4) Dispatcher operation: If, in a stable state, no branch exceeds short-term overload limit, the dispatcher intervenes to relieve overloads by either adjusting generation outputs or disconnecting units and loads. This action is modeled via DCOPF, details can be found in [15]. The procedure estimates the ultimate lost load during an event, obviating the need for more detailed AC models at this stage.

5) Over- and under-excitation: To maintain terminal voltage stability under varying conditions, generators adjust excitation current but are subject to thermal and stability limits. These constraints lead to an interconversion between PV and PQ bus types depending on whether the reactive power limits are binding. This switching mechanism is realized through (7).

B. Detailed Simulation Procedure

Beyond the linear AC power-flow calculation and the protection/control mechanism simulations described above, the cascading failure model also incorporates an islanding detection routine based on breadth-first search. Starting from the initial contingency set and grid state, the model executes simulations and outputs cascading propagation paths, and lost load. For detailed simulation procedure, see Fig. 1.

IV. Case Study

This section validates the advantages of the proposed model through comparisons of power flow calculations and cascading outcomes. The comparative analysis was performed in MATLAB with the aid of MATPOWER 8.1, with detailed protection parameters adopted from [11].

A. Accuracy and Efficiency of the Linear AC Power Flow

In this section, the performances of different power flow calculation methods are compared, to demonstrate the accuracy and efficiency of the proposed linear AC power flow.

The error distributions for voltage magnitude and branch loading rate are analyzed in Fig. 2 and 3, given their critical

979-8-3315-8138-1

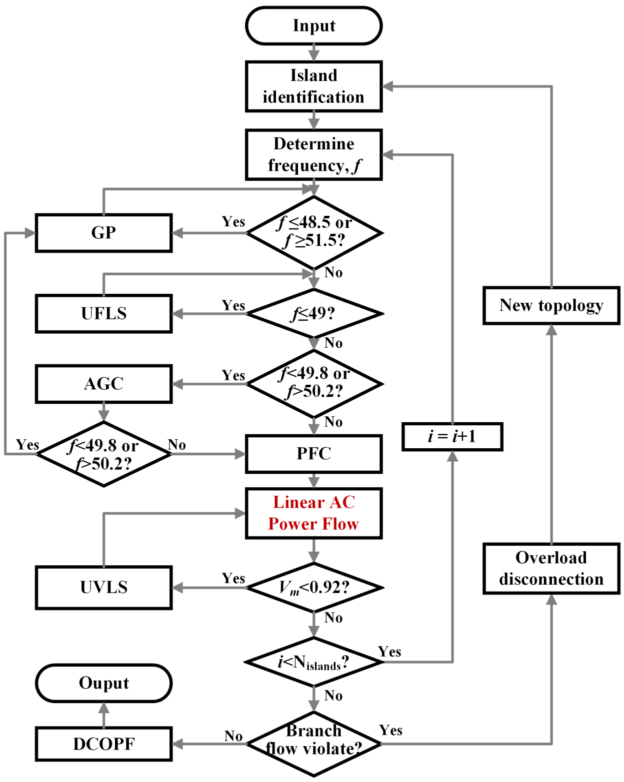

Fig. 1. Flowchart of the proposed cascading failure model

role in the propagation of cascading failures. Across all test systems, the branch loading rate estimation error exhibits almost unbiased normal distribution characteristics, with the values consistently bounded within 10% and the vast majority falling below 4%, thereby demonstrating high accuracy. Furthermore, the voltage magnitude estimation errors are predominantly within 0.02 p.u. In contrast, the DC power flow fails to capture the voltage distribution, with errors increasing as the system voltage range widens.

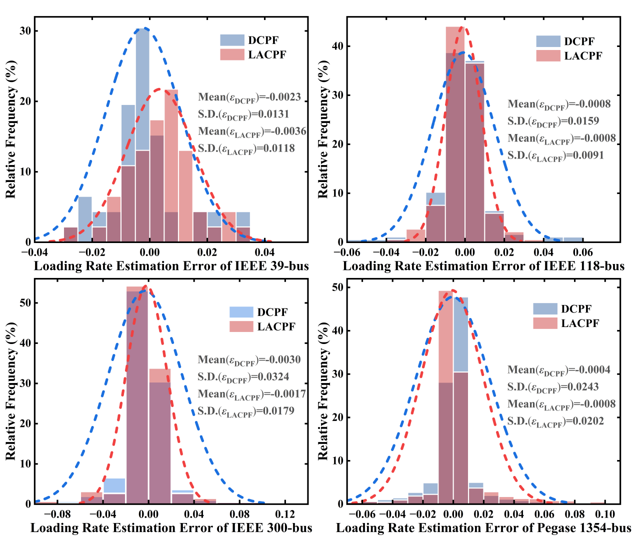

Fig. 2. Branch loading rate estimation error

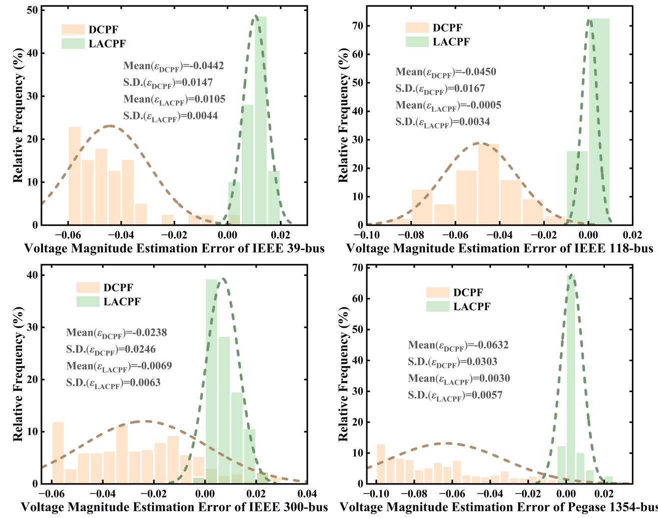

Fig. 3. Voltage magnitude estimation error

It is worth noting that such accuracy is well-suited for cascading failure analysis, which permits a broader error tolerance. Since NERC Standard PRC-023-1 mandates relay settings of no less than 115% of the emergency rating [16], a safety margin of at least 15% is inherently available. Given that the model's errors fall safely within this margin, setting the threshold at the emergency rating allows for the conservative identification of potential branch trips without omission.

To validate the model's robustness under extreme conditions, its performance under extremely heavy loading scenarios was tested, as shown in Fig. 4. The branch loading rate estimation error of the proposed model remains within 15%, with the vast majority falling below 8%, demonstrating high accuracy. Furthermore, the voltage magnitude estimation errors are predominantly within 0.02 p.u. The error analysis suggests that the proposed model is capable of maintaining high accuracy even under deteriorated operating conditions.

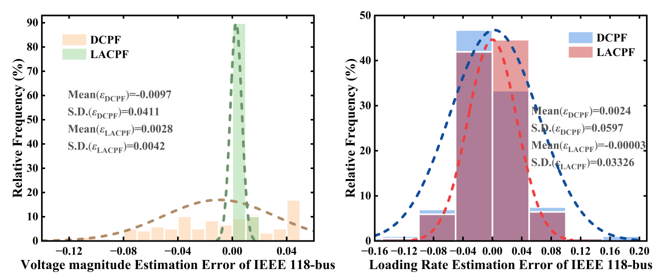

Fig. 4. Estimation error under extreme heavy loading

Furthermore, a comparison of computational efficiency across benchmark systems is provided in Tab. II. Owing to sparse matrix structures and the absence of iterative procedures, the proposed linear AC power flow model delivers at least twofold speedup over ACPF and ACOPF, even on large-scale systems. This efficiency gain significantly accelerates cascading-failure simulations, where power flow calculations constitute a major computational burden.

979-8-3315-8138-1

TABLE II
COMPARISON OF THOUSAND-TIME COMPUTATION TIME

Test Systems	Thousand-Time Computation Time / s			
	ACPF	*DCPF*	*ACOPF*	*LACPF*
IEEE 39-bus	9.57	7.66	53.96	0.23
IEEE 118-bus	11.47	9.24	63.24	0.55
IEEE 300-bus	22.11	9.71	144.83	1.96
Pegase 1354-bus	35.12	12.65	1341.04	17.05

B. Comparative Analysis of Cascading Failure Models

The models are evaluated on the IEEE 118-bus system using an initial contingency set generated via Monte Carlo simulation with identical branch failure probabilities. The complementary cumulative distribution functions (CCDF) of lost load plotted on double logarithm axes are shown in Fig. 5. The simulation data generated by the proposed model aligns well with the historical trends of power law distributions observed in statistical studies [17].

Compared to the DC power-flow-based model, our inclusion of under-voltage load shedding leads to higher lost load and a right-shifted distribution curve. This result is physically rational, as it captures the aggravating effect of voltage violation that DC models inherently underestimate. Conversely, optimization-based load shedding benefit from idealized decision-making to yield lower lost load and a flatter tail, while rigid uniform load shedding schemes exhibit tail inflections, highlighting that rigid adjustment may trigger more total blackouts. While strictly validating which model better represents reality is challenging, our comparative results demonstrate a degree of physical plausibility. Moreover, by reverting load-shedding decisions to the actual physical processes, our approach offers enhanced interpretability. However, the linear model inherently bypasses physical non-convergence issues. This limitation suggests a potential underestimation of system collapse risks.

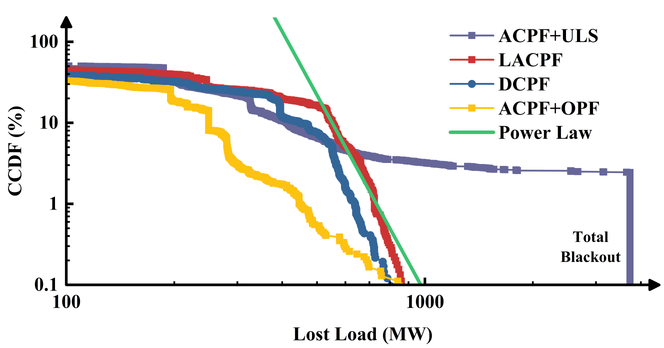

Fig. 5. Complementary cumulative distribution functions for lost load

V. CONCLUSION

This paper proposes a simplified AC power flow model that delivers accurate voltage estimates while retaining linear and sparse calculation matrices for efficiency and robust convergence. Validated on benchmark systems, the power flow achieves voltage magnitude errors within 2% and provides at least a twofold speedup. Building on this, a cascading failure model with detailed modeling of protection and control mechanisms is established. The framework executes load shedding on stable power flow solutions, avoiding heuristics commonly used to bypass non-convergence. Validated on IEEE 118-bus system, the approach mitigates the overestimation from rigid uniform load shedding and the underestimation from rational OPF-based load shedding.

REFERENCES

[1] Yujia Li, Shunbo Lei, Wei Sun, Chenxi Hu, and Yunhe Hou. A distributionally robust resilience enhancement strategy for distribution networks considering decision-dependent contingencies. *IEEE Transactions on Smart Grid*, 15(2):1450–1465, March 2024.

[2] Mathaios Panteli and Pierluigi Mancarella. Modeling and evaluating the resilience of critical electrical power infrastructure to extreme weather events. *IEEE Systems Journal*, 11(3):1733–1742, September 2017.

[3] Byungkwon Park, Xiaowen Su, and Kai Sun. An enhanced opa model: Incorporating dynamically induced cascading failures. *IEEE Transactions on Power Systems*, 37(6):4962–4965, 2022.

[4] Jiajia Song, Eduardo Cotilla-Sanchez, Goodarz Ghanavati, and Paul D. H. Hines. Dynamic modeling of cascading failure in power systems. *IEEE Transactions on Power Systems*, 31(3):2085–2095, May 2016.

[5] Xiaoyu Zheng, Hitoshi Tamaki, Tomoyuki Sugiyama, and Yu Maruyama. Dynamic probabilistic risk assessment of nuclear power plants using multi-fidelity simulations. *Reliability Engineering & System Safety*, 223:108503, July 2022.

[6] Wenyun Ju, Kai Sun, and Rui Yao. Simulation of cascading outages using a power-flow model considering frequency. *IEEE Access*, 6:37784–37795, 2018.

[7] Rui Yao, Shaowei Huang, Kai Sun, Feng Liu, Xuemin Zhang, and Shengwei Mei. A multi-timescale quasi-dynamic model for simulation of cascading outages. *IEEE Transactions on Power Systems*, 31(4):3189–3201, July 2016.

[8] Yitian Dai, Matthias Noebels, Mathaios Panteli, and Robin Preece. Evaluating the effect of dynamic and static modelling on cascading failure analysis in power systems. In *2021 IEEE Madrid Powertech*, pages 1–6, June 2021.

[9] Pierre Henneaux, Emanuele Ciapessoni, Diego Cirio, Eduardo Cotilla-Sanchez, Ruisheng Diao, Ian Dobson, Anish Gaikwad, Stephen Miller, Milorad Papic, Andrea Pitto, Junjian Qi, Nader Samaan, Giovanni Sansavini, Sunitha Uppalapati, and Rui Yao. Benchmarking quasi-steady state cascading outage analysis methodologies. In *2018 IEEE International Conference on Probabilistic Methods Applied to Power Systems (PMAPS)*, pages 1–6, 2018.

[10] Jian Li, Leonardo Dueñas-Osorio, Changkun Chen, and Congling Shi. AC power flow importance measures considering multi-element failures. *Reliability Engineering & System Safety*, 160:89–97, April 2017.

[11] Matthias Noebels, Robin Preece, and Mathaios Panteli. AC cascading failure model for resilience analysis in power networks. *IEEE Systems Journal*, 16(1):374–385, March 2022.

[12] Xuan Liu and Zuyi Li. Revealing the impact of multiple solutions in DCOPF on the risk assessment of line cascading failure in OPA model. *IEEE Transactions on Power Systems*, 31(5):4159–4160, September 2016.

[13] Jingwei Yang, Ning Zhang, Chongqing Kang, and Qing Xia. A state-independent linear power flow model with accurate estimation of voltage magnitude. *IEEE Transactions on Power Systems*, 32(5):3607–3617, September 2017.

[14] O. Alizadeh Mousavi, M. Bozorg, R. Cherkaoui, and M. Paolone. Inter-area frequency control reserve assessment regarding dynamics of cascading outages and blackouts. *Electric Power Systems Research*, 107:144–152, 2014.

[15] Xiaoguang Wei, Shibin Gao, Tao Huang, Ettore Bompard, Renjian Pi, and Tao Wang. Complex network-based cascading faults graph for the analysis of transmission network vulnerability. *IEEE Transactions on Industrial Informatics*, 15(3):1265–1276, March 2019.

[16] Liang Che, Xuan Liu, Yunfeng Wen, and Zuyi Li. Identification of cascading failure initiated by hidden multiple-branch contingency. *IEEE Transactions on Reliability*, 68(1):149–160, 2019.

[17] Paul Hines, Jay Apt, and Sarosh Talukdar. Large blackouts in north america: Historical trends and policy implications. *Energy Policy*, 37(12):5249–5259, 2009.

979-8-3315-8138-1